Zeros of the Husimi function and quantum numbers in the HCP molecule

Article *in* The European Physical Journal D · November 2010

Impact Factor: 1.23 · DOI: 10.1140/epjd/e2010-00228-y

4 authors:

Francisco Javier Arranz
Universidad Politécnica de Madrid
34 PUBLICATIONS **175** CITATIONS
SEE PROFILE

Zaki Safi
Al-Azhar University - Gaza
19 PUBLICATIONS **42** CITATIONS
SEE PROFILE

Rosa M Benito
Universidad Politécnica de Madrid
173 PUBLICATIONS **999** CITATIONS
SEE PROFILE

Florentino Borondo
Universidad Autónoma de Madrid
157 PUBLICATIONS **1,645** CITATIONS
SEE PROFILE

Eur. Phys. J. D **60**, 279–286 (2010)
DOI: 10.1140/epjd/e2010-00228-y

THE EUROPEAN PHYSICAL JOURNAL D

Regular Article

Zeros of the Husimi function and quantum numbers in the HCP molecule

F.J. Arranz[1,2,a], Z.S. Safi[3,b], R.M. Benito[1,4,c], and F. Borondo[3,5,d]

[1] Grupo de Sistemas Complejos, Universidad Politécnica de Madrid, 28040 Madrid, Spain
[2] Departamento de Ingeniería Rural, E.T.S.I. Agrónomos, Universidad Politécnica de Madrid, 28040 Madrid, Spain
[3] Departamento de Química, Universidad Autónoma de Madrid, Cantoblanco, 28049 Madrid, Spain
[4] Departamento de Física, E.T.S.I. Agrónomos, Universidad Politécnica de Madrid, 28040 Madrid, Spain
[5] Instituto Mixto de Matemáticas CSIC–UAM–UC3M–UCM, Universidad Autónoma de Madrid, Cantoblanco, 28049 Madrid, Spain

Received 7 May 2010
Published online 8 September 2010 –

Abstract. The feasibility of using the zeros of the Husimi function to characterize, i.e. ascribe quantum numbers to, dynamical systems with mixed dynamics is explored using a realistic model for the vibrations of the HCP molecule as an example. Further implications are also discussed.

1 Introduction

The correspondence between classical and quantum mechanics has been a topic of much interest, specially in the context of quantum chaos [1]. It was Niels Bohr that made the first attempt to solve this problem by enunciating a correspondence principle [2,3], that only tackled the problem partially. Later, it was realized that for systems with fully integrable dynamics this correspondence is well understood in terms of the celebrated Einstein-Brillouin-Keller (EBK) quantization rule [4–6] for the classical trajectory actions, I_j,

$$\oint_{\mathcal{C}_j} \boldsymbol{P}\cdot d\boldsymbol{q} = 2\pi\hbar\left(n_j+\frac{\alpha_j}{4}\right), \qquad n_j = 0,1,2,\ldots \tag{1}$$

These integrals should be computed, according to Einstein's prescription, which corrected Bohr's simpler view, on the N (this being the dimension of the problem) topologically independent paths, $\mathcal{C}_j$, defining the invariant tori [7] on which the motion can take place. Parameters α_j are known as the Maslov indices [8], which take care of the topological phase accumulated along the circuits [10][1]. Equation (1) constitutes a true semiclassical expression in which a quantum condition involving integer quantum numbers (r.h.s.) is imposed to purely classical information (l.h.s). Moreover, for each allowed energy in (1) there is an associated wave function, as shown by Wentzel, Kramers and Brillouin (WKB) [5],

$$\psi_{WKB}(\boldsymbol{q}) = \sum_j A_j \exp\left[\frac{iS_j(\boldsymbol{I},\boldsymbol{q})}{\hbar}\right], \tag{2}$$

where $S_j(\boldsymbol{I},\boldsymbol{q})$ are the branches of the Hamilton's characteristic function solving the Hamilton-Jacobi equation [11].

Numerous strategies have been reported in the literature to solve equation (1). Among them, probably the most intuitive and straightforward one is that due to Noid and Marcus [12], which obtained the quantized energies by direct numerical construction of the invariant tori. It is also worth mentioning here the adiabatic switching method[2], which is based in the preservation of the action under adiabatic perturbations on the Hamiltonian. This idea, originally due to Ehrenfest [14] and Einstein [15], was applied in the 1980's to the semiclassically quantization of nonintegrable systems [16–20], covering different aspects of the problem.

Interestingly enough, Einstein's paper on the quantization of tori [4] contains a remarkable little comment at the end. In it, he pointed out towards the problem arising when the system is nonintegrable and the associated motion becomes irregular. Enstein knew of Poincaré's work on the three body problem and the possibility of chaos [21] in dynamical systems, that was later later developed with the publication of the

[a] e-mail: fj.arranz@upm.es
[b] *Permanent address*: Department of Chemistry, Faculty of Science, Al-Azhar University of Gaza, P.O. Box 1277, Palestine.
[c] e-mail: rosamaria.benito@upm.es
[d] e-mail: f.borondo@uam.es

[1] Maslov index is easily understood in one dimensional systems, where the topological phase is picked up only at the turning points due to the discontinuity induced by the momentum passing through zero. See for example: [9].

[2] See for example review in [13].

Kolmogorov-Arnold-Moser (KAM) theorem [22]. But the question remained untouched, largely because of the great success of the new quantum mechanics, until the 1970's in which Martin Gutzwiller tackled the problem of quantizing classically chaotic systems with his celebrated trace formulae [23,24]. Starting from the expression of the full quantum propagator, Gutzwiller was able to make a semiclassical approximation for the trace, containing only information concerning (all) the periodic orbits (POs) of the system. Due to the exponential proliferation of such special orbits with the excitation energy the expression is difficult, if not impossible, to apply, except for very simple or special problems [25,26]. Gutzwiller's trace formula showed for the first time the relevance of POs in the quantum dynamics of chaotic systems, and other works continued progressing along this line. Among them, those concerning the so called scar theory should be mentioned here [27,28].

In 1984, Eric Heller showed for the first time that some individuals eigenfunctions of classically chaotic systems present a strong localization of the probability density along POs [29]. Later, Bogolmony [30] studied this scarring phenomena as an emergent property in groups of eigenstates [31–33].

Another way to asses the quantum relevance of particular classical structures, such as invariant tori, POs, etc. [31–35], is the construction of quantum analogues to the surface of section (SOS). In classical mechanics Poincaré was the first to discuss the efficiency of this method to reveal the dynamical information contained in the phase space of mechanical systems [21]. Classically, composite SOS are easily obtained by projecting a swarm of trajectories, all propagated at the same energy, into specific surfaces in phase space. A widespread method to obtain the quantum mechanical analogous phase space density distributions is due to Wigner, who proposed the following expression [36,37]

$$\mathcal{W}(\boldsymbol{P},\boldsymbol{q}) = \frac{1}{2\pi\hbar^N}\int d\boldsymbol{x}\; e^{i\boldsymbol{P}\cdot\boldsymbol{q}/\hbar}\;\psi^*\left(\boldsymbol{q}-\frac{\boldsymbol{x}}{2}\right)\;\psi\left(\boldsymbol{q}+\frac{\boldsymbol{x}}{2}\right), \tag{3}$$

$|\psi\rangle$ being the wavefunction of the system. One popular alternative is the Husimi function [38] or coherent state representation, given by

$$\mathcal{H}(\boldsymbol{P},\boldsymbol{q}) = |\langle\phi_{\boldsymbol{P},\boldsymbol{q}}|\psi\rangle|^2, \tag{4}$$

where $\phi_{\boldsymbol{P},\boldsymbol{q}}$ represents a harmonic oscillator coherent state [39]. Expression (4) can be shown to be equal to a Gaussian smoothed Wigner function, right in the spirit of the Heisenberg uncertainty principle. From either of these two functions, Wigner or Husimi, quantum analogues (QSOS) to the SOS devised by Poincaré can be defined. The comparison of these two complementary constructions have allowed for a long time the study of the correspondence between quantum and classical mechanics. Typically, the Wigner and Husimi functions usually appear peaked on classical structures with quantum relevance [31–35].

Much less studied are the zeros of the Husimi function, despite the fact that, since this function is a positive defined one, they can provide, in principle, a complete characterization of it. This procedure was originally suggested by Leboeuf and Voros [40–42], who found in two dimensional maps that every pure quantum state admits a finite multiplicative parametrization by the zeros of its Husimi function. For pure eigenstates the distribution of these zeros in phase space explicitly reflects the nature of the underlying classical dynamics. In the semiclassical regime the distribution becomes one dimensional for integrable systems, while it spreads out for chaotic systems [43–51]. A good review of this topic can be found in reference [52]. These authors coined the term 'stellar representation' to refer to this set of points, which can be used as a minimal set encoding the corresponding states.

In this paper we seek to study the practical feasibility of using the zeros of the Husimi function, or rather of in the associated QSOS, to study the characteristics of some molecular states, with the future aim of using them to unveil subtle information contained in it; see for example [31–33].

As an example to illustrate our points, we choose to study the vibrational dynamics of the HCP molecule described by a reduced dimensionality (2dof) realistic model, that has been introduced previously by us [53]. With it, we were able to show the relevant dynamical information in the chaotic sea using a local frequency analysis [54,55]. The results of this analysis was compared with results obtained from Poincaré SOS.

The organization of the paper is as follows. In Section 2.1 we describe the system under study, and review the computational procedure used. Numerical results are presented and discussed in Section 3. Finally, in Section 4 we summarize the main conclusions derived from our work.

2 System and calculations

2.1 The HCP molecular system

The system that we choose to study is a reduced dimensionality model for the vibrations of the HCP molecule, that has been studied previously [53] to get an overall idea of the phase space structure (mainly detection of regular and chaotic motions) for the vibrational dynamics of this system. It consists of a 2 degrees of freedom model, in which the C–P bond is hold frozen at a distance of $r_e = 3.01003$ a.u. Although this approximation ignores the Fermi resonance existing between the bending and the C–P motion [56,57], it is certainly good enough for the purposes of the present paper (see also discussion in Ref. [53]).

The HCP potential energy surface (PES), responsible for the forces acting on the atoms, has been taken from the literature. It consists of a fitting [58] to data obtained by a sophisticated CASSCF [59,60] quantum calculation to the following analytical expression

$$V = V_1(1-\lambda_1) + V_2\lambda_1 - \delta V\lambda_2 + V_0, \tag{5}$$

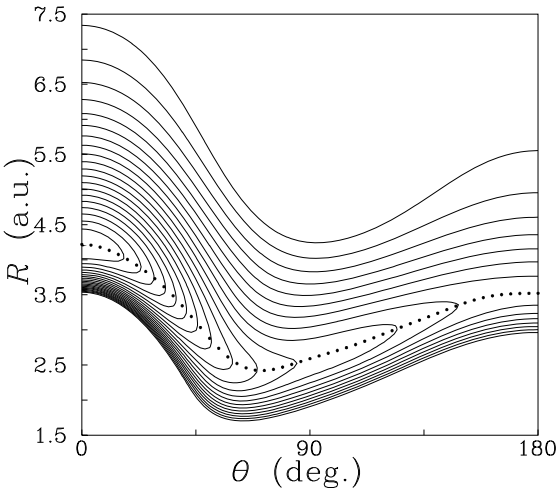

Fig. 1. Potential energy surface for HCP as function of R and θ for a fixed value of $r_{CP} = 3.01003$ a.u. Contours are separated by 1008 cm^{-1} with a maximum value of 40 327 cm^{-1} above the minimum. The minimum energy path, connecting the HCP well and the saddle point, is shown superimposed as a dotted line.

where a good accuracy was achieved by optimizing the terms V_1 and V_2 respectively for two different ranges of energy, one going up to 18 150 cm^{-1} above the minimum of the PES, and the other for energies above this value. The proper connection between these two regimes is obtained by the use of the two energy-dependent switching functions, λ_1 and λ_2, given by

$$\lambda_1 = \frac{1 + \tanh[4(V_2 + 3.0)]}{2},$$
$$\lambda_2 = \frac{1 + \tanh[12(V_2 + 1.3)]}{2}. \quad (6)$$

The constant term, V_0, in equation (5) is chosen so that the energy at the minimum coincides with the value, $-42\,230$ cm^{-1}, of older versions of the potential considered in references [61,62], and δV is a correction term [63].

This PES is presented as a contours plot in Figure 1. As can be seen, it presents a potential well at $\theta = 0°$, corresponding to the linear configuration H–CP. The other linear configuration, $\theta = 180°$, corresponds to a saddle point with an associated barrier of 27 358 cm^{-1}. Thus, at energies above this value, the H atom may sample large portions of the PES, thus giving rise to vibrational chaos. Superimposed to the PES in Figure 1, the minimum energy path, $R_e(\theta)$, going from the minimum to the saddle has also been plotted in dotted line. It is given by the following Fourier series,

$$\begin{aligned} R_e(\theta) = {} & 3.186460 + 0.123553\ \cos\theta + 0.679693\ \cos 2\theta \\ & + 0.239818\ \cos 3\theta + 0.034727\ \cos 4\theta \\ & - 0.045755\ \cos 5\theta - 0.039552\ \cos 6\theta \\ & - 0.001833\ \cos 7\theta + 0.013533\ \cos 8\theta \\ & + 0.017138\ \cos 9\theta \end{aligned} \quad (7)$$

in atomic units.

The classical vibrational ($J = 0$) Hamiltonian function is given by

$$H = \frac{P_R^2}{2\mu_{\mathrm{H-CP}}} + \frac{1}{2}\left(\frac{1}{\mu_{\mathrm{H-CP}}R^2} + \frac{1}{\mu_{\mathrm{C-P}}r_e^2}\right)P_\theta^2 + V(R,\theta), \quad (8)$$

where R is the distance from the center of mass of the CP fragment to the H atom, θ is the angle between the C–P and the R vectors, and P_R and P_θ are the associated conjugate momenta. The corresponding reduced mass are defined as follows:

$$\mu_{\mathrm{H-CP}} = \frac{m_H(m_C + m_P)}{m_H + m_C + m_P}$$
$$\mu_{\mathrm{C-P}} = \frac{m_C m_P}{m_C + m_P} \quad (9)$$

where m_H, m_C and m_P are the masses of hydrogen, carbon and phosphorus atoms, respectively.

2.2 Computational procedure

The vibrational dynamics of this system has been studied by classical trajectory calculations. For this purpose Hamilton's equations of motion derived from equation (8) have been numerically integrated using a Gear algorithm. To monitor the vibrational dynamics undertaken by the system and visualize its phase space structure Poincaré SOS have been computed for each trajectory. An adequate choice for this, namely one giving the most meaningful dynamical information, is the intersection with the minimum energy path, $R_e(\theta)$. To make this chosen SOS an area preserving map, we need also to perform the following canonical transformation [64]

$$\begin{aligned} \rho &= R - R_e(\theta), \\ \vartheta &= \theta, \\ P_\rho &= P_R, \\ P_\vartheta &= P_\theta + \left(\frac{dR_e}{d\theta}\right)P_R. \end{aligned} \quad (10)$$

The SOS condition is now given by expression $\rho = 0$, complemented with the condition that P_ρ is in a predetermined branch (the negative one in our case) of the second degree equation obtained from energy conservation. It is also important to fold this SOS into the $0 \le \theta \le \pi$ interval using invariance under the transformations $\vartheta \to 2\pi - \vartheta$ and $P_\vartheta \to -P_\vartheta$ for reasons that will be explained below when describing the quantum calculations.

2.3 Quantum dynamics

For the quantum calculations we have used the DVR–DGB program of Bacic and Light [65] to obtain the first 100 vibrational eigenfunctions $\langle R, \theta | n \rangle$ with the corresponding eigenenergies converged to within 0.01 cm^{-1}. Although more converged states can be easily obtained

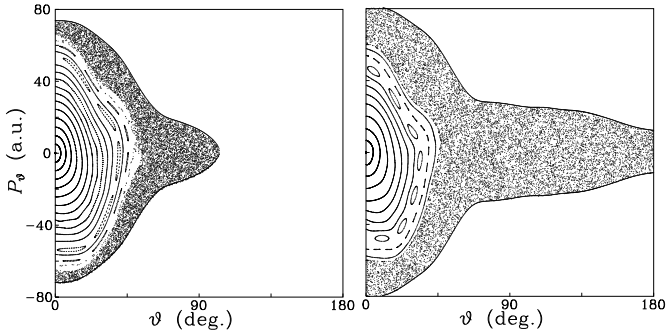

Fig. 2. Poincaré surfaces of section as defined in Section 2.2 for the vibrational dynamics of our 2D model for HCP at 22.395 (left) and 27.381 cm^{-1} (right), respectively.

this is enough for the purposes of the present paper. The corresponding Husimi functions or coherent-state representation,

$$\mathcal{H}_n(R,\theta,P_R,P_\theta) = \frac{1}{(2\pi\hbar)^2}\left|\langle R,\theta,P_R,P_\theta|n\rangle\right|^2, \qquad (11)$$

where $|R,\theta,P_R,P_\theta\rangle$ is a harmonic-oscillator coherent state, have also been calculated by direct numerical integration [64]. In our case, and in order to be able to compare with the classical results, we have considered Husimi-based QSOS [64], $\mathcal{H}_n^{\mathrm{QSOS}}(\vartheta,P_\vartheta)$, carrying out the change of variables in equation (10) over the Husimi function $\mathcal{H}_n(R,\theta,P_R,P_\theta)$, and using the same definition described above for the classical SOS, i.e. $\rho = 0$ and P_ρ in a predetermined branch of the momentum function. Moreover, the corresponding results will be presented in the folded fashion described for the classical counterpart in the previous section in order to reconcile the quantum with the classical results. Indeed and, as it is well known, for total $J = 0$, the quantum dynamics of a linear triatomic molecule presents a zero probability in the linear configuration [66]. On the other hand, the corresponding classical dynamics is planar, thus not precluding this conformation. This issue was first discussed by Watson [67], who proposed a dynamical way to avoid the problem which consistent with our simpler folding procedure. The zeroes of this function are calculated using the procedure described in reference [68].

3 Results

3.1 Classical dynamics

We start this section by presenting our results concerning the classical vibrational dynamics of our model for HCP. Some Poincaré SOS for two different values of the excitation energy are shown in Figure 2. The results presented in the left panel correspond to $E_{\mathrm{vib}} = 22.395$ cm^{-1}, an energy slightly below the barrier for the HPC unstable (saddle of the PES) linear configuration. At this value of the energy, the system presents a clear mixed dynamical regime, where regions of regularity (around the H–CP well) coexist with a small region of chaos that is observed in the outer region of the SOS, especially close to the boundaries. In the regular region it is obvious the presence of two resonances. The most conspicuous one is seen as a chain of islands corresponding to the 2:10 resonance that appear close to the chaotic region. The other one, that it is also observed at lower energies, corresponds to a 2:16 resonance but the associated chain of island which are located at smaller values of the angular coordinate, θ, is unfortunately too narrow to be seen in the scale of the figure. The right panel shows the results corresponding to $E_{\mathrm{vib}} = 27.381$ cm^{-1}, a bigger energy above the saddle point of the PES. The dynamics here are more chaotic, especially in the tube connecting the two linear configurations, and this is noticed in the SOS that presents a larger region of irregularity. The regular portion of the phase space appears accordingly much reduced, and here a 2:14 resonance is visible.

Table 1. Eigenenergies corresponding to the states presented in Figures 3–5.

n	E_{vib} (cm^{-1})	(n_R, n_θ)
1	0	(0, 0)
2	1248.8	(0, 2)
3	2495.2	(0, 4)
4	3227.4	(1, 0)
5	3736.4	(0, 6)
6	4450.3	(1, 2)
7	4969.4	(0, 8)
8	5668.8	(1, 4)
9	6191.5	(0, 10)
10	6326.8	(2, 0)
11	6880.4	(1, 6)
12	7936.6	(0, 12)

3.2 Quantum results

We start this subsection by presenting respectively in Table 1 and Figure 3 the eigenenergies and eigenfunctions of the first twelve states of the HCP model. As can be seen, all wavefunctions look very regular in the sense that they present a very clear and well defined nodal pattern. Actually, quantum numbers can be easily and unambiguously ascribed to all of them in a coordinate system consisting of the MEP and the direction perpendicular to it. The corresponding assignments of vibrational states has been added as the last column to Table 1. Notice that in the notation here we have approximated the corresponding coordinate system to simply (R,θ).

The corresponding Husimi-based QSOS are shown in Figure 4. Consequent with the simple structure shown by the HCP eigenfunctions, the QSOS present also an structure easy to interpret. In particular, it can be seen that all QSOS corresponding to states of the type $(n_R, 0)$, that is states number $n = 1$, 4 and 10, appear centered at the origin, where they show a big maximum. For states excited along the angular coordinate, i.e. $n_\theta \neq 0$ the structure gets more complicated. Essentially, the quantum quasi-probability density accumulates, for these states, along the boundaries of the available phase space. But there also appear a number of zeros in the inner part.

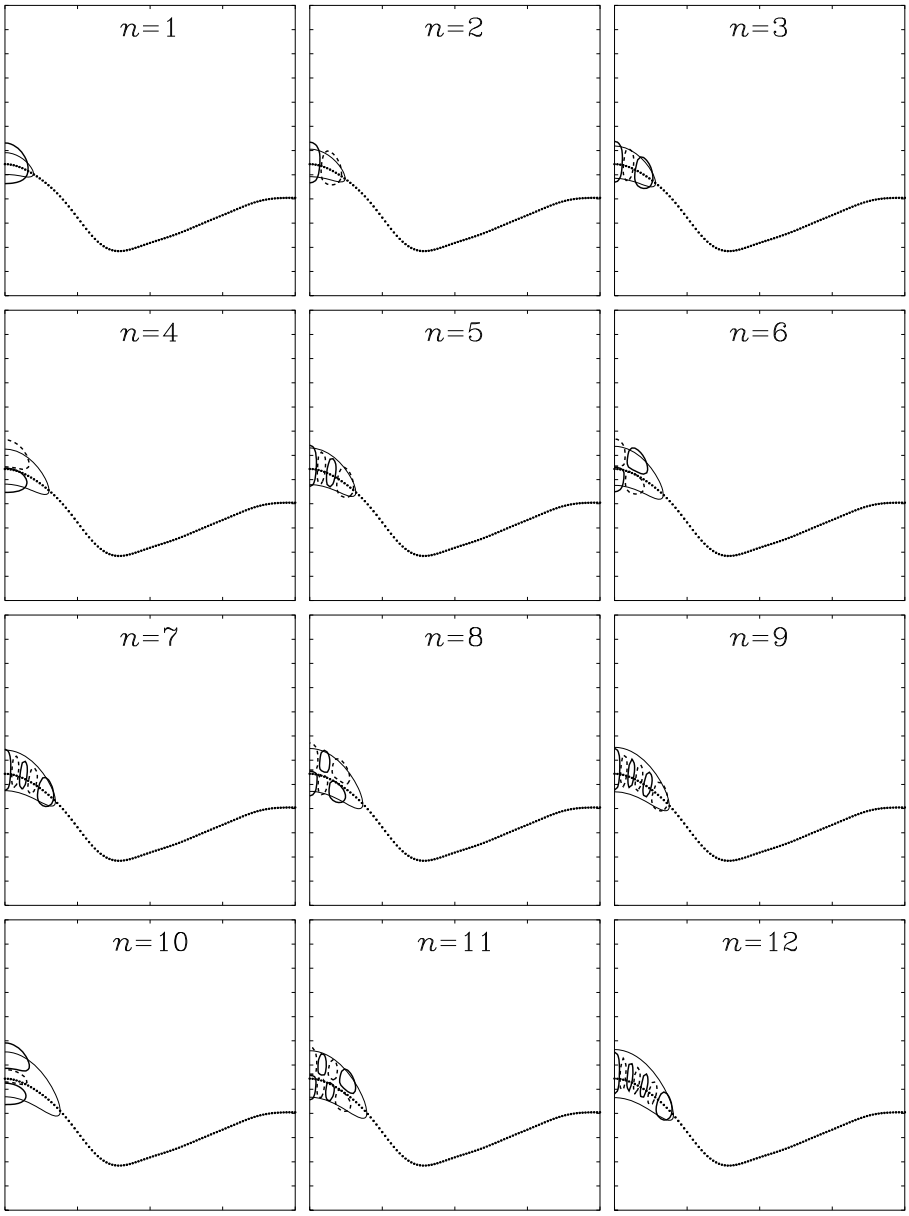

Fig. 3. Eigenfunctions for the first twelve states of our model for HCP.

To discuss in more detail the physics associated with these zeros, we have accurately computed [68] their locations, and the results are shown in Figure 5. As can be seen one finds in all plots a number of zeros coincident with the quantum number along the MEP, that we have notated in an approximated way as n_ϑ. Namely, none for states $n = 1, 4$ and 10 for which $n_\vartheta = 0$, one for states $n = 2$ and 6 for which $n_\vartheta = 1$, two for states $n = 3$ and 8 for which $n_\vartheta = 2$, three for states $n = 5$ and 11 for which $n_\vartheta = 3$, four for state $n = 7$ for which $n_\vartheta = 4$, five for state $n = 9$ for which $n_\vartheta = 5$, and six for state $n = 12$ for which $n_\vartheta = 6$. The conclusion is that for molecular Hamiltonian systems like the one we are considering the zeros of the Husimi function, projected here onto one of the possible QSOS, seems to be a good criterium to organize the quantum states, in agreement with the conclusions of Voros and coworkers in their papers on the stellar representation [52].

One final comment is in order here before closing this section. In our discussion we have only used the first twelve vibrational states of HCP, a number that may seem meager at first sight. However, we have done this just for simplicity, since there are any other states with completely similar characteristics to those presented here in the hundredth that we have considered. Actually, one can make this argument more quantitative and state that among the set of eigenstates computed by us 67 of them fall into this category of what can be called regular states, the corresponding quantum numbers ranging from $n_R =$ 0–6 and $n_\vartheta =$ 0–20. The rest of interleaved states present a more irregular and unassignable structure of the quantum probability density.

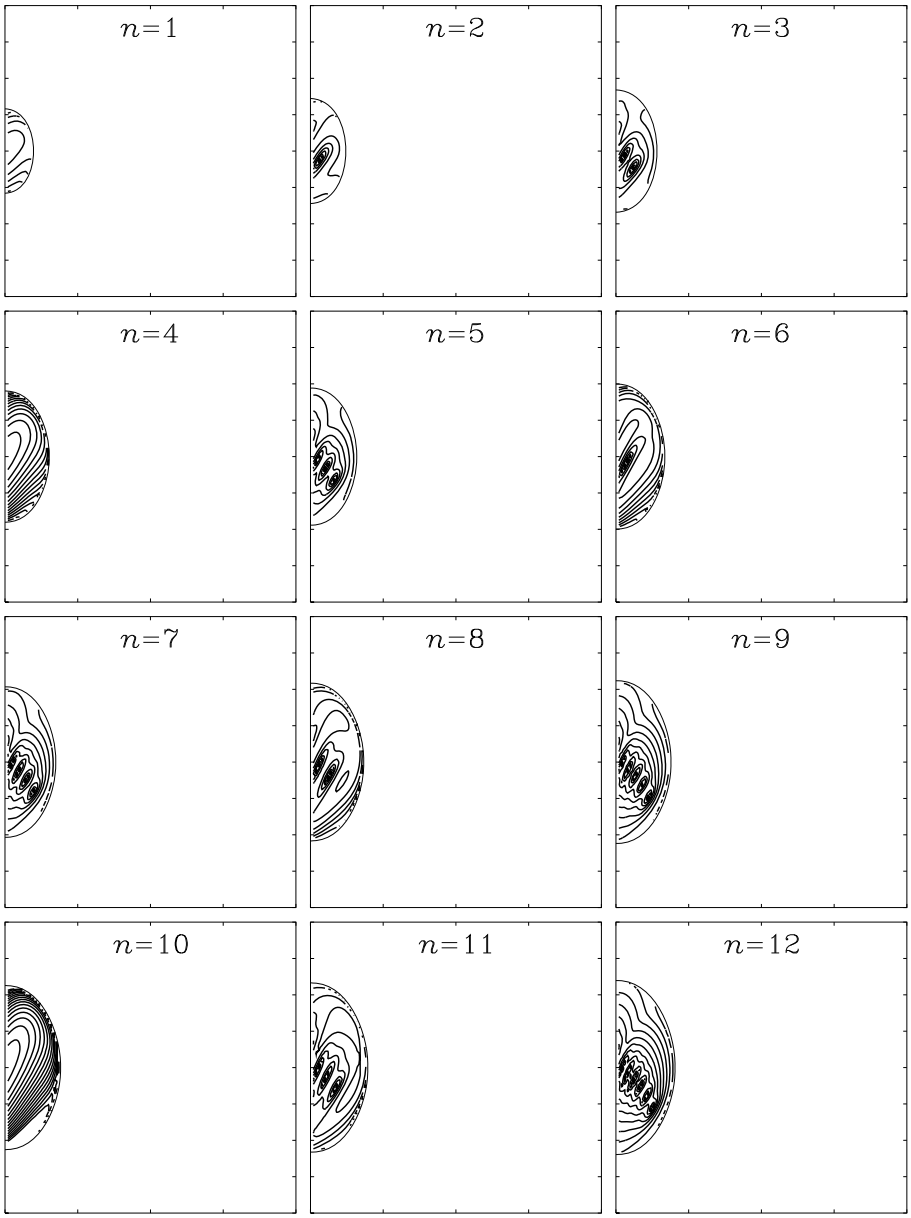

Fig. 4. Husimi-based quantum surfaces of section corresponding to the first twelve states of our model for HCP.

4 Summary

We have studied for the first time the distribution of zeros corresponding to the vibrational dynamics of the HCP molecule. For this purpose we have used a realistic model with the dimensionality reduced to two degrees of freedom introduced in a previous publication. The results obtained in our numerical study indicate that these zeros can be used to fully characterized (at least) the regular quantum states, as suggested by Voros and coworkers in their work on the stellar representation [52]. Moreover, they coincide in this case very accurately with the position of the intersection of the nodal planes with the MEP, i.e. with the surface used in our calculations to construct the classical and quantum SOSs.

These are important results since they will be used in the future to explore other characteristics of quantum states which are more subtle [69]. Namely, we plan to use this method in the future to study in more detail the relevance of homoclinic and heteroclinic quantized circuits in the eigenfunctions. We have already shown the relation of such circuits with spectral and Husimi properties of scarred states on classically chaotic systems [31–35]. Using the Voros's stellar representation we think that it should be possible to introduce new quantum numbers related with these circuits, following an idea put forward by Ozorio de Almeida some time ago [70].

Support from MICINN-Spain under contract No. MTM2009-14621 and i-MATH CSD2006-32, and Comunidad de Madrid under contract SIMUMAT S-0505/ESP-0158, is gratefully acknowledged.

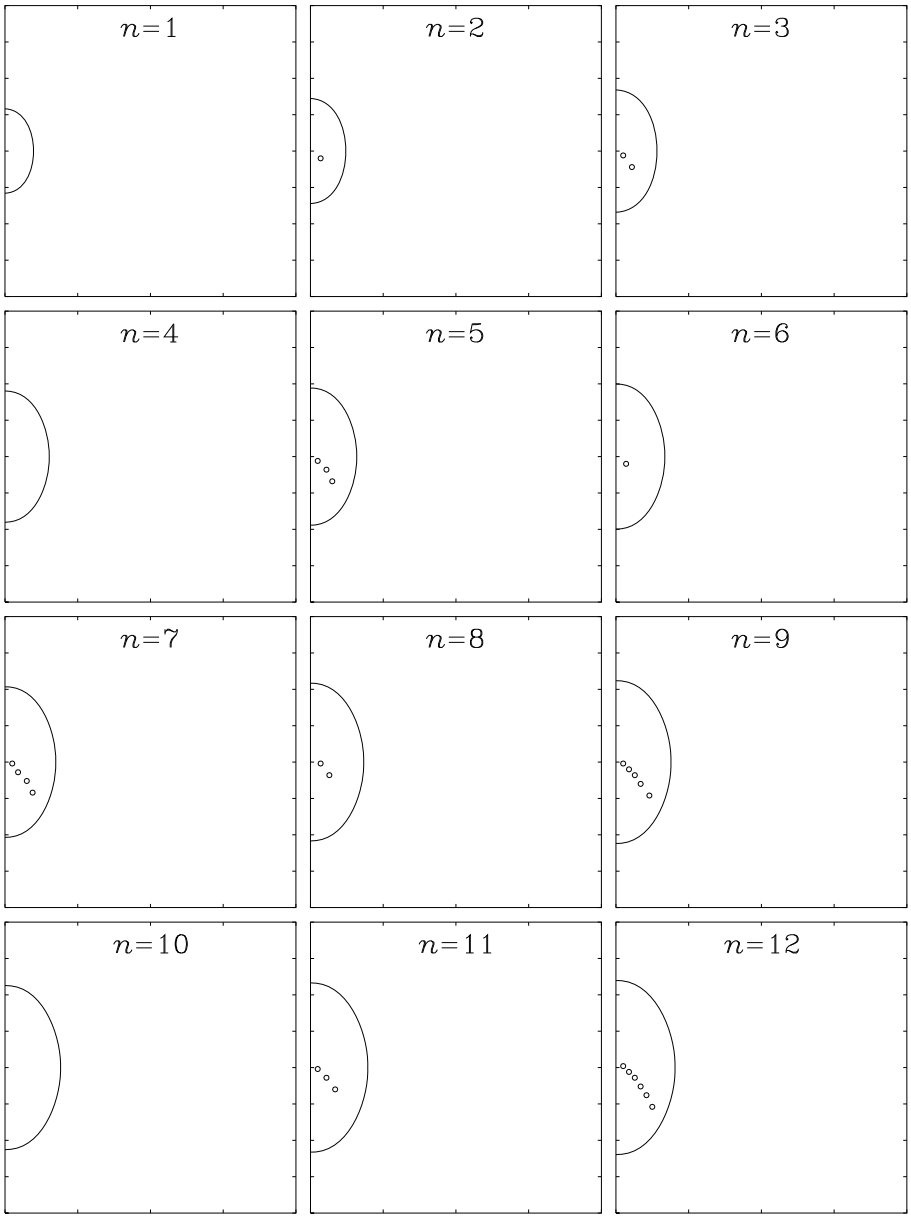

Fig. 5. Location of the zeros of the Husimi-based quantum surfaces of section corresponding to the first twelve states of our model for HCP.

References

1. M.C. Gutzwiller, *Chaos in Classical and Quantum Mechanics* (Springer-Verlag, New York, 1990)
2. N. Bohr, Phil. Mag. **2**, 1 (1913)
3. *Sources of Quantum Mechanics*, edited by B.L. van der Waerden (Dover, New York, 1967)
4. A. Einstein, Verh. Dtsch. Phys. Ges. **19**, 82 (1917)
5. M.L. Brillouin, J. Phys. Radium **7**, 353 (1926)
6. J.B. Keller, Ann. Phys. NY **4**, 180 (1958)
7. A.J. Lichtenberg, M.A. Lieberman, *Regular and Chaotic Dynamics* (Springer Verlag, New York, 1992)
8. V. Maslov, M.V. Feodoriuk, *Semiclassical Approximations in Quantum Mechanics* (Reidel, Boston, 1981)
9. L.D. Landau, E.M. Lifshitz, *Quantum Mechanics: Non-Relativistic Theory* (Pergamon Press, Oxford, 1977)
10. M. Brack, R.K. Bhaduri, *Semiclassical Physics* (Addison-Wesley, Reading, MA, 1997)
11. H. Goldstein, C.P. Poole, J.L. Safko, *Classical Mechanics*, 3rd edition (Addison Wesley, New York, 2002)
12. D.W. Noid, R.M. Marcus, J. Chem. Phys. **62**, 2119 (1975)
13. F. Borondo, *Computational Chemistry: Structure, Interactions and Reactivity*, Part A, edited by S. Fraga (Elsevier, Amsterdam, 1992), and references therein
14. P. Ehrenfest, Verslagen Kon. Akad. Amsterdam **25**, 412 (1916). An agridged English translation is found in reference [3], p. 72
15. A. Einstein, in *La Théorie du rayonnement et les quanta. Rapports du discussions de la réunion tenue à Bruxelles*, edited by P. Langevin, L. de Broglie (Gauthiers-Villars, Paris, 1912), p. 450

16. R.M. Hedges, R.T. Skodje, F. Borondo, W.P. Reinhardt, ACS Symp. Ser. **263**, 323 (1984)
17. R.T. Skodje, F. Borondo, W.P. Reinhardt, J. Chem. Phys. **82**, 4611 (1985)
18. R.T. Skodje, F. Borondo, Chem. Phys. Lett. **118**, 409 (1985)
19. R.T. Skodje, F. Borondo, J. Chem. Phys. **84**, 1533 (1986)
20. R.T. Skodje, F. Borondo, J. Chem. Phys. **85**, 2760 (1986)
21. H. Poincaré, *Les Méthodes Nouvelles de la Mécanique Céleste* (Gauthiers-Villars, Paris, 1899)
22. J. Pöschel, Proc. Symp. Pure Math. **69**, 707 (2001)
23. M.C. Gutzwiller, J. Math. Phys. **10**, 1004 (1969)
24. M.C. Gutzwiller, J. Math. Phys. **11**, 1791 (1970)
25. M.C. Gutzwiller, J. Math. Phys. **14**, 139 (1973)
26. R. Prosmiti, S.C. Farantos, R. Guantes, F. Borondo, R.M. Benito, J. Chem Phys. **104**, 2921 (1996)
27. E.J. Heller, in *1989 NATO Les Houches Summer School on Chaos and Quantum Physics*, edited by M-J. Giannoni, A. Voros, J. Zinn-Justin (Elsevier, Amsterdam, 1991)
28. L. Kaplan, E.J. Heller, Ann. Phys. **264**, 171 (1998)
29. E.J. Heller, Phys. Rev. Lett. **53**, 1515 (1984)
30. E.B. Bogomolny, Physica D **31**, 169 (1988)
31. D. Wisniacki, E. Vergini, R.M. Benito, F. Borondo, Phys. Rev. Lett. **94**, 054101 (2005)
32. F. Borondo, E. Vergini, D. Wisniacki, A.A. Zembekov, R.M. Benito, J. Chem. Phys. **122**, 111101 (2005)
33. D. Wisniacki, E. Vergini, R.M. Benito, F. Borondo, Phys. Rev. Lett. **97**, 094101 (2006)
34. E.L. Sibert III, E. Vergini, R.M. Benito, F. Borondo, New J. Phys. **10**, 053016 (2008)
35. E.G. Vergini, E.L. Sibert III, F. Revuelta, R.M. Benito, F. Borondo, Europhys. Lett. **89**, 40013 (2009)
36. E. Wigner, Phys. Rev. **40**, 749 (1932)
37. J.E. Moyal, Proc. Cambridge Phil. Soc. **45**, 99 (1949)
38. K. Husimi, Proc. Phys. Soc. Jpn **22**, 264 (1940)
39. J.P. Gazeau, *Coherent States in Quantum Physics* (Wiley-VCH, Berlin, 2009)
40. P. Leboeuf, A. Voros, J. Phys. A **23**, 1765 (1990)
41. P. Leboeuf, J. Phys. A **24**, 4575 (1991)
42. M.B. Cibils, Y. Cuche, P. Leboeuf, W.F. Wreszinski, Phys. Rev. A **46**, 4560 (1992)
43. J.-M. Tualle, A. Voros, Chaos **5**, 1085 (1995)
44. F.J. Arranz, R.M. Benito, F. Borondo, Phys. Rev. E **54**, 2458 (1996)
45. H. Wiescher, H.J. Korsch, J. Phys. A **30**, 1763 (1997)
46. F.J. Arranz, R.M. Benito, F. Borondo, J. Mol. Struct. -Theochem **426**, 87 (1998)
47. D. Biswas, S. Sinha, Phys. Rev. E **60**, 408 (1999)
48. H.J. Korsch, C. Müller, H. Wiescher, J. Phys. A **30**, L677 (1997)
49. T. Prosen, J. Phys. A **29**, 5429 (1996)
50. P. Toscano, A.M. Ozorio de Almeida, J. Phys. A **32**, 6321 (1999)
51. F.J. Arranz, R.M. Benito, F. Borondo, J. Chem. Phys. **120**, 6516 (2004)
52. S. Nonnenmacher, A. Voros, J. Stat. Phys. **92**, 431 (1998)
53. Z.S. Safi, J.C. Losada, R.M. Benito, F. Borondo, J. Chem. Phys. **129**, 164316 (2008)
54. J.C. Losada, J.M. Estebaranz, R.M. Benito, F. Borondo, J. Chem. Phys. **108**, 63 (1998)
55. J.C. Losada, R.M. Benito, F. Borondo, Eur. Phys. J. Special Topics **165**, 183 (2008)
56. H. Ishikawa, R.W. Field, S.C. Farantos, M. Joyeux, J. Koput, C. Beck, R. Schinke, Ann. Rev. Phys. Chem. **50**, 443 (1999)
57. M. Joyeux, S.Y. Grebenshchikov, J. Bredenbeck, R. Schinke, S.C. Farantos, Adv. Chem. Phys. **130A**, 267 (2005), and references therein
58. C. Beck, R. Schinke, J. Koput, J. Chem. Phys. **112**, 8446 (2000)
59. H.-J. Werner, P.J. Knowles, J. Chem. Phys. **82**, 5053 (1985)
60. P.J. Knowles, H.-J. Werner, Chem. Phys. Lett. **115**, 259 (1985)
61. S.C. Farantos, H.–M. Keller, R. Schinke, K. Yamashita, K. Morokuma, J. Chem. Phys. **104**, 10055 (1996)
62. C. Beck, H.-M. Keller, S.Y. Grebenshchikov, R. Schinke, S.C. Farantos, K. Yamashita, K. Morokuma, J. Chem. Phys. **107**, 9818 (1997)
63. Q. Wu, J.Z.H. Zhang, J.M. Bowman, J. Chem. Phys. **107**, 3602 (1997)
64. R.M. Benito, F. Borondo, J.H. Kim, B.G. Sumpter, G.S. Ezra, Chem. Phys. Lett. **161**, 60 (1989)
65. Z. Bacic, J.C. Light, Ann. Rev. Phys. Chem. **40**, 469 (1989)
66. See for example: I.N. Levine, *Molecular Spectroscopy* (John Wiley, New York, 1975)
67. J.K.G. Watson, J. Chem. Phys. **90**, 6443 (1989)
68. F.J. Arranz, R.M. Benito, F. Borondo, J. Chem. Phys. **120**, 6516 (2004)
69. E.G. Vergini, R.M. Benito, F. Borondo (in preparation)
70. A.M. Ozorio de Almeida, Nonlinearity **2**, 519 (1989)